Applied Food Research 6 (2026) 101913



Contents lists available at ScienceDirect

Applied Food Research

journal homepage: www.elsevier.com/locate/afres



Detecting wheat flour adulteration by portable infrared and Raman spectroscopies

Abimbola Oluwakayode [a], Joe Stradling [b], Angel Medina [a], Rudolf Krska [c,d], Royston Goodacre [b,*]

[a] Magan Centre of Applied Mycology, Cranfield University, College Rd. Wharley End, Bedford MK43 0AL, UK
[b] Centre for Metabolomics Research, Department of Biochemistry, Cell and Systems Biology, Institute of Systems, Molecular and Integrative Biology, University of Liverpool, Liverpool L69 7ZB, United Kingdom
[c] Institute for Global Food Security, National Measurement Laboratory, Centre of Excellence in Agriculture and Food Integrity, Queen's University Belfast, 19 Chlorine Gardens, Belfast BT9 5DL, UK
[d] BOKU University, Department of Agricultural Sciences, Institute of Bioanalytics and Agro-Metabolomics, Konrad-Lorenz, Str. 20, 3430, Tulln, Austria

ARTICLE INFO

Keywords:
Wheat flour adulteration
Portable spectroscopy
Raman spectroscopy
Infrared spectroscopy
Food fraud detection

ABSTRACT

Monitoring wheat flour fraud is vital, especially during global disruptions like the war in Ukraine, which heighten the risk of economically motivated adulteration. This study explores the use of portable Raman and infrared (IR) spectroscopy to detect wheat flour adulteration with potato and corn flour. Principal Component Analysis (PCA) revealed spectral differences, while Partial Least Squares Regression (PLSR) models quantified adulterant levels. Both techniques successfully identified adulteration, with typical errors of prediction for test samples of 4–5 % for infrared and 8.7–10.6 % for Raman spectroscopy. In addition, IR achieved a limit of detection (LOD) as low as 6.9 % and Raman 22.6 %. The findings highlight portable vibrational spectroscopy as a rapid, non-destructive tool for detecting flour fraud, supporting food quality control and regulatory enforcement

1. Introduction

Food adulteration refers to the intentional compromise of food quality through the addition of harmful, lower-quality, or non-authentic substances, which can render the food unsafe, misleading, or nutritionally inferior (Choudhary et al., 2020; Ellis et al., 2012). This practice poses serious health risks, ranging from mild digestive issues to severe illnesses, including acute anaphylaxis and long-term diseases like cancer (Bansal et al., 2017; Meghwal et al., 2022). Foods that are particularly vulnerable to adulteration include honey, milk, vegetable oils, spices, beverages, meat, and flours (Essuman et al., 2022; Narayan, 2014; Tomar & Alka, 2022). Flour is a finely ground powder produced by milling grains, seeds, or root crops, serving as a fundamental ingredient in a wide range of food products. It provides structure, texture, and stability in baked goods, sauces, and processed foods. Wheat flour is the leading choice in baking and food production, driven by its widespread availability and strong consumer preference. Its dominance exceeds alternatives like corn and potato flour, which are typically reserved for specialised applications. Flour, being a vital ingredient in many diets globally, is increasingly targeted for adulteration. Research has uncovered a variety of deceptive practices including the addition of chalk, starch, and non-food grade chemicals, which compromise product quality and mislead consumers. These adulterants are often difficult to detect through visual inspection alone, as the structure of the grain/-seed/tuber is not evident after milling. Beyond diminishing the nutritional value of flour, they also pose significant health risks, especially to vulnerable groups such as children and the elderly.

The problem of flour adulteration, specifically wheat flour, is expected to worsen due to ongoing global challenges such as climate change and geopolitical instability. Climate change is increasingly disrupting wheat production by intensifying droughts, heatwaves, and extreme weather events, leading to reduced yields and lower-quality harvests (Faller et al., 2021). The war in Ukraine has further intensified these challenges by disrupting one of the world's largest wheat supply chains. As a result, the area of land harvested for wheat in Ukraine fell from 7.0 million hectares in 2020–2021 to just 4.2 million hectares in 2023–2024 (Reliefweb, 2024). Countries that rely heavily on wheat imports, particularly in Africa, the Middle East, and parts of Asia,

* Corresponding author.
E-mail addresses: abimbola.oluwakayode@cranfield.ac.uk (A. Oluwakayode), j.stradling@liverpool.ac.uk (J. Stradling), a.medinavaya@cranfield.ac.uk (A. Medina), rudolf.krska@boku.ac.at (R. Krska), roy.goodacre@liverpool.ac.uk (R. Goodacre).

https://doi.org/10.1016/j.afres.2026.101913
Received 27 October 2025; Received in revised form 9 March 2026; Accepted 17 March 2026
Available online 18 March 2026
2772-5022/© 2026 The Author(s). Published by Elsevier B.V. This is an open access article under the CC BY license (http://creativecommons.org/licenses/by/4.0/).

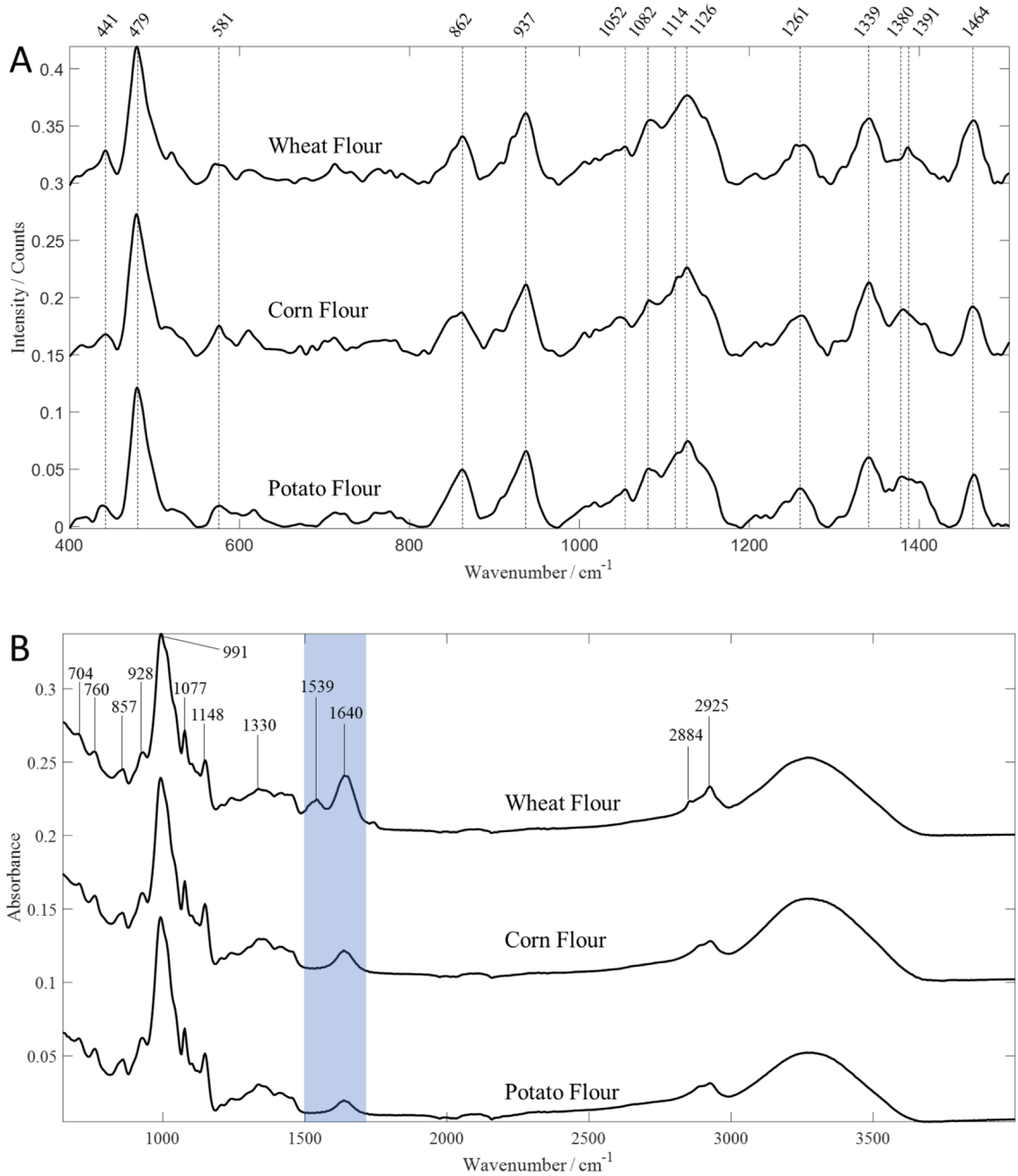


Fig. 1. Raman (A) and Infrared (B) spectra of wheat flour, corn flour and potato flour, with dominant bands highlighted and tentatively assigned in Tables 1 and 2.

are struggling to secure stable supplies, making them more vulnerable to fraudulent or substandard flour entering the market. In regions with weak regulatory oversight, the demand-supply imbalance creates an environment where economically motivated adulteration, such as the addition of lower-cost starches, chalk, or even hazardous substances, becomes more prevalent. As a result, a proactive approach is essential to prevent emerging fraud trends, such as the illicit addition of less in-demand flours.

Detection techniques for flour adulteration have evolved to include sophisticated analytical methods such as chromatography and spectroscopy, aimed at identifying specific contaminants and quantifying their presence accurately. Mass spectroscopy (MS) (Chien et al., 2023), gas chromatography (GC) (Pastor et al., 2019), and high-performance liquid chromatography (HPLC) (Sahu et al., 2020) are commonly employed for detecting food adulteration. However, these methods have specific drawbacks, including challenges in sampling, time consumption, generation of toxic waste, the high maintenance costs associated with the equipment, as well as the need to ship the sample to the instrument.

In contrast, Raman spectroscopy offers a rapid, reliable, cost-effective, and non-destructive method for detecting food adulterants. Its capacity for real-time analysis, combined with the availability of compact, portable (handheld) instruments, makes it an ideal tool for monitoring food quality across a wide range of production environments, storage facilities, and agricultural settings. These advantages make Raman spectroscopy a uniquely effective tool for proactive food safety monitoring (Stradling et al., 2024). Complementary to Raman spectroscopy, and available as a portable (handheld) technique, Fourier transform infrared (FT-IR) spectroscopy is another widely used method for analysing the biochemical profiles of biological samples. While Raman spectroscopy probes the vibrational modes of Raman-active biomolecules - such as proteins, nucleic acids, carbohydrates, and

Table 1
Typical Raman band and assignments associated with wheat four.

Wavenumber (cm^{-1})	Tentative assignments taken from Czaja et al. (2020) and Stawoska et al. (2021)
441	Polysaccharides (skeletal mode of pyranose ring)
479	Polysaccharides (marker band to identify presence of starch)
581	Polysaccharides (C-H)
862	Mono-, di- and polysaccharides (stretching or deformation modes referring to the glycosidic bond)
937	Polysaccharides (marker band for glycosidic linkage observed in starch)
1052	Polysaccharides
1082	Polysaccharides
1114	C-O stretching and C-H bending modes in polysaccharides
1126	Polysaccharides
1261	Polysaccharides, lipids and fatty acids
1339	Polysaccharides, lipids and fatty acids
1380	Polysaccharides (deformation modes)
1391	Starch (C-C-H bending)
1464	Polysaccharides, lipids and fatty acids

Table 2
Typical infrared band regions and assignments associated with similar four.

Wavenumber Range (cm^{-1})	Tentative assignments taken from Arslan et al. (2020)
4000–3025	(O-H) stretching
3025–2800	(C-H and N-H) stretching
1835–1585	β sheet of amide I, (COH, CCH, OCH, and C-O) stretching
1585–1495	β sheet of amide II
1495–1280	(C-H, N-H, and C-H) stretching and bending vibration
1280–1220	β sheets of amide III (N-H and C-H) stretching and bending vibration
1220–950	(C-O and C-C) bending vibration
950–885	(COH, CCH, OCH and C-O) stretching and bending vibration
885–450	(COH, CCH and OCH) stretching vibration

lipids - via inelastic light scattering to provide molecular-specific information, infrared spectroscopy exploits the absorption of IR-active vibrational modes in the same classes of biomolecules. (Baker et al., 2014). Both spectroscopic methods have been recently applied to detect food adulteration in flours (Li et al., 2024; Lohumi et al., 2019; Ziegler et al., 2016). These portable capable guardians allow on site analyses (Ellis et al., 2016) and when combined with chemometrics, their performance in identifying food adulterants is further enhanced (Oliveira et al., 2020; Sezer et al., 2022; Unuvar et al., 2023).

Food adulteration is typically motivated by economic gain, often involving the substitution of higher-value ingredients with cheaper alternatives. However, in some cases, more expensive flours like corn or potato may be used to adulterate wheat flour - particularly when demand for those flours is low or when wheat prices are high or supply is limited. In such situations, blending in potato or corn flour can increase production volume and lower overall costs. Whilst the addition of potato or corn flour may offer functional advantages for non-celiac gluten-intolerant individuals, undisclosed adulteration compromises product authenticity and poses challenges for food quality control. Besides, potato flour has a similar starch composition to wheat flour, making it difficult to distinguish between the two without advanced analytical methods (AzoMaterials, 2023).

This study assessed for the first time the effectiveness of *portable* Raman and FT-IR spectroscopic methods, in conjunction with chemometric techniques such as PCA and PLS-R, to detect and predict varying levels of potato and corn flour adulteration in wheat flour.

2. Materials and methodology

2.1. The flour

Wheat grains, corn flour and potato flour branded by Buy Wholefoods Online (Bwfo) were purchased from an online retailer. The wheat grains were ground with an electric coffee grinder (MCG-1830A, Hong Kong). Flour from the lid compartment was obtained as a flour texture similar to corn and potato flour.

Flour particle size was determined using a static light scattering (SLS) Mastersizer (Materials Innovation Factory (MIF), Liverpool, United Kingdom). See Figure S1 in the Supplementary Information. The particle sizes for all three flour types were similar. The particle size distributions of all three flour types were broadly similar. Wheat flour exhibited a bimodal distribution with peaks around 10 μm and 100 μm, spanning a wide range from 2 to 700 μm. Corn flour particles had a mean diameter of approximately 10 μm, with sizes ranging from 5 to 110 μm. Potato flour particles were generally larger, with a mean diameter of 40 μm and a range between 10 and 100 μm.

2.2. Spectroscopic analysis

2.2.1. Raman spectroscopy

In this study, corn and potato flour were used as adulterants of wheat flour. Samples were prepared by weighing 300 mg into glass vials, consisting of either pure corn, potato, or wheat flour, or mixtures of two flours of wheat with either potato or wheat with corn flour, with adulteration levels ranging from 5 % to 95 % in 5 % increments. Five samples were prepared for each adulteration level, and three spectra were recorded for each sample (ensuring the samples were vortexed for 5 s after each measurement) resulting in 15 spectra per adulteration level.

Raman spectra were collected from all samples using a CBEx handheld Raman spectrometer (Snowy Range, Laramie, Wyoming, USA) using a 1064 nm laser with a typical power on the sample of ~30 mW. Spectral datasets were recorded in the 400 to 2300 cm^{-1} spectral range with an acquisition time of 15 s. The measurements were performed by placing the glass vial containing each sample into the sample holder (vial-mode).

2.2.2. FT-IR spectroscopy

The same samples used in the Raman measurements were used for FT-IR analysis. As with the Raman spectral collection, three FT-IR spectra were collected from each sample (resulting in 15 spectra per each adulteration level) using an Agilent Cary 630 FTIR spectrometer (5301 Stevens Creek Blvd, Santa Clara, CA 95,051, United States) equipped with a diamond-ATR (attenuated total reflectance). A background scan was performed to eliminate the absorption from the environment or the flour matrix. For each sample, a small amount of the vortexed flour was placed on the sample holder. The hydraulic press of the FT-IR was pressed against the flour to form a thin pellet, and the spectra were recorded using 32 sample scans with a spectral range between 650 and 4000 cm^{-1} and a resolution of 8 cm^{-1}.

2.2.3. Data analysis

Following data collection, all spectral analysis was carried out in Matlab R2022a (The Mathworks, Natick, MA, USA). PCA was applied to visualise the relationship between the Raman and FT-IR data. Prior to PCA, Raman spectra were first baseline corrected using asymmetric least squares, smoothed with a Savitzky–Golay filter with a 2nd order polynomial and a window width of 11 points and vector normalised, whilst for FT-IR the data were just vector normalised (Gautam et al., 2015; Savitzky & Golay, 1964).

PLS-R was employed to quantitatively model and predict the various levels of adulteration. For all Partial Least Squares Regression (PLS-R) analysis, spectra were vector normalised only, with no further preprocessing which could lead to overfitting of the data. To construct

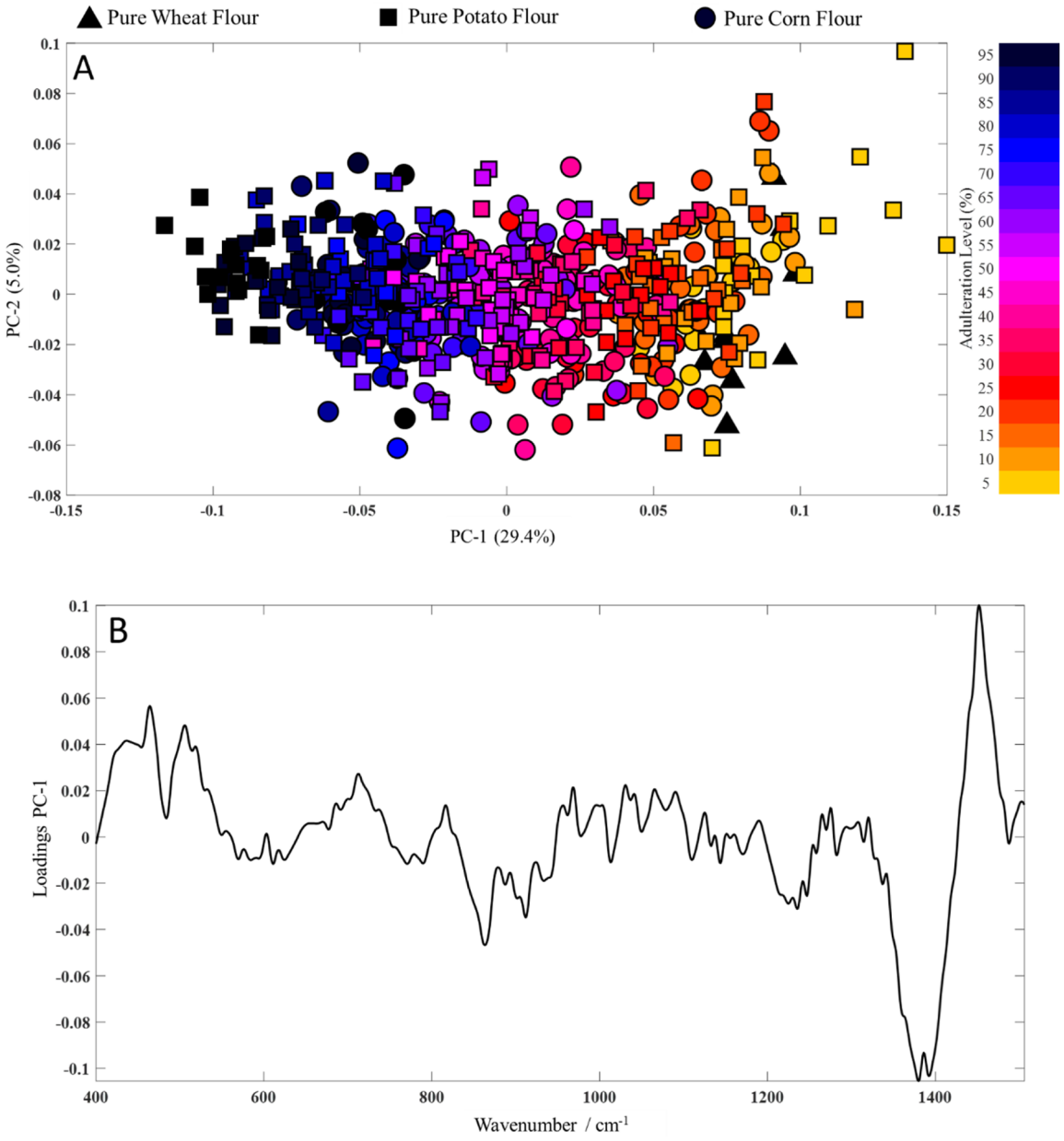


Fig. 2. PCA scores plot illustrating the differentiation of wheat flour samples adulterated with varying levels of potato and corn flour, based on Raman spectroscopy data (A). Associated PC-1 loadings plot (B).

the PLS-R models, training data consisted of adulteration levels ranging from 0 % to 100 % in 10 % increments, while the test data included adulteration levels of 5 % to 95 % in 10 % increments for each corn and potato adulterants in wheat flour.

In addition, to test the robustness of the PLS-R models a series of 20 "blind" samples were generated. In this case the adulteration levels were known to the researcher generating the samples (A.O.), but not to the researcher who collected the IR and Raman data and performed the data analysis to predict the adulteration levels for the 20 samples (J.S.). For each blind sample three Raman spectra and three FT-IR spectra were recorded. The PLS-R model was then used to predict the levels of adulteration for these unknown samples.

3. Results

3.1. Raman and IR spectroscopy of the flours

The Raman and FT-IR spectra of wheat, corn, and potato flours are expected to show notable similarities, primarily due to the presence of starch, the dominant carbohydrate in all three crops. Starch, consisting of the polysaccharides amylose and amylopectin, contributes to characteristic vibrational features in both Raman and IR spectra, such as C-O stretching and C-H bending vibrations (Fig. 1; Tables 1 and 2). These starch-related features are similar across the flours, as the starch molecules share a comparable structure. While differences in protein and lipid content exist between the flours, the predominant influence of starch on their spectra overshadows these variations. As a result, despite minor spectral differences linked to protein and lipid composition, the overall spectral patterns of wheat, corn, and potato flours remain largely analogous (Fig. 1).

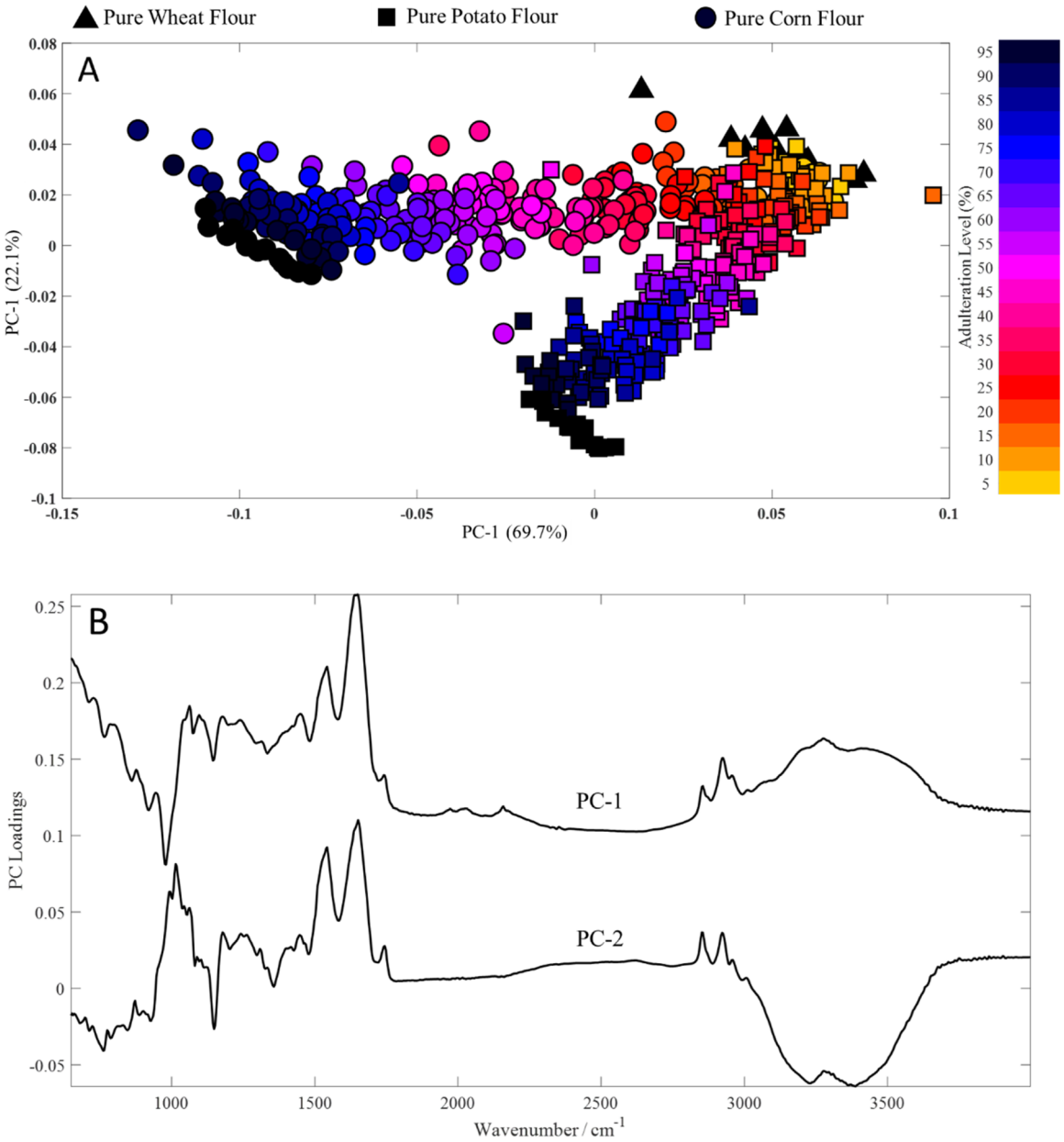


Fig. 3. PCA scores plot illustrating the differentiation of wheat flour samples adulterated with varying levels of potato and corn flour, based on infrared spectroscopy data (A). Associated PC-1 and PC-2 loadings plots (B).

The Raman spectra of all three flours (Fig. 1A) exhibit a high degree of similarity, again primarily due to the dominant presence of starch, with slight variations and relatively low protein contents across the flours; wheat flour (starch: 70–75 %, protein: 8–16 %) (Van Hung et al., 2006), potato flour (starch: ~83 %, protein: 6–10 %) (Buzera et al., 2023; King Arthur Baking, 2017), and corn flour (starch: 75–87 %, protein: 6–8 %) (Arendt & Dal Bello, 2008). This suggests that the spectral features associated with proteins are overshadowed by the stronger bands corresponding to starch (assigned in Table 1).

In IR spectroscopy, proteins display strong absorption bands, particularly in the amide I, II, and III regions, due to dipole moment changes associated with vibrational modes such as C═O stretching, N-H bending, and C-N stretching. These absorption bands are generally more intense and easier to detect compared to the typically weaker Raman scattering signals. As a result, although the spectra of wheat, corn, and potato flours are similar, slight differences in the protein-associated bands can be observed (Fig. 1B and Table 2). One notable difference is the presence of a band at 1539 cm^{-1} in the spectrum of wheat flour. This band corresponds to the amide II region and, while not a protein itself, reflects specific vibrational motions within the protein molecules. It is associated with N-H bending and C-N stretching vibrations in the peptide bonds of proteins, which are characteristic of the protein structure and commonly observed in the IR spectrum of proteins. Additionally, differences in the intensity of peaks at 1640 cm^{-1} (associated with amide I) are evident, with wheat flour showing the highest intensity peak. This is expected given that wheat flour contains a higher protein content compared to corn and potato flours.

3.2. *Principal component analysis*

The above spectra are all very similar and only show subtle differences between them. Chemometric techniques offer powerful tools for visualising and discriminating between complex data sets, especially in cases where differences are not readily apparent through visual

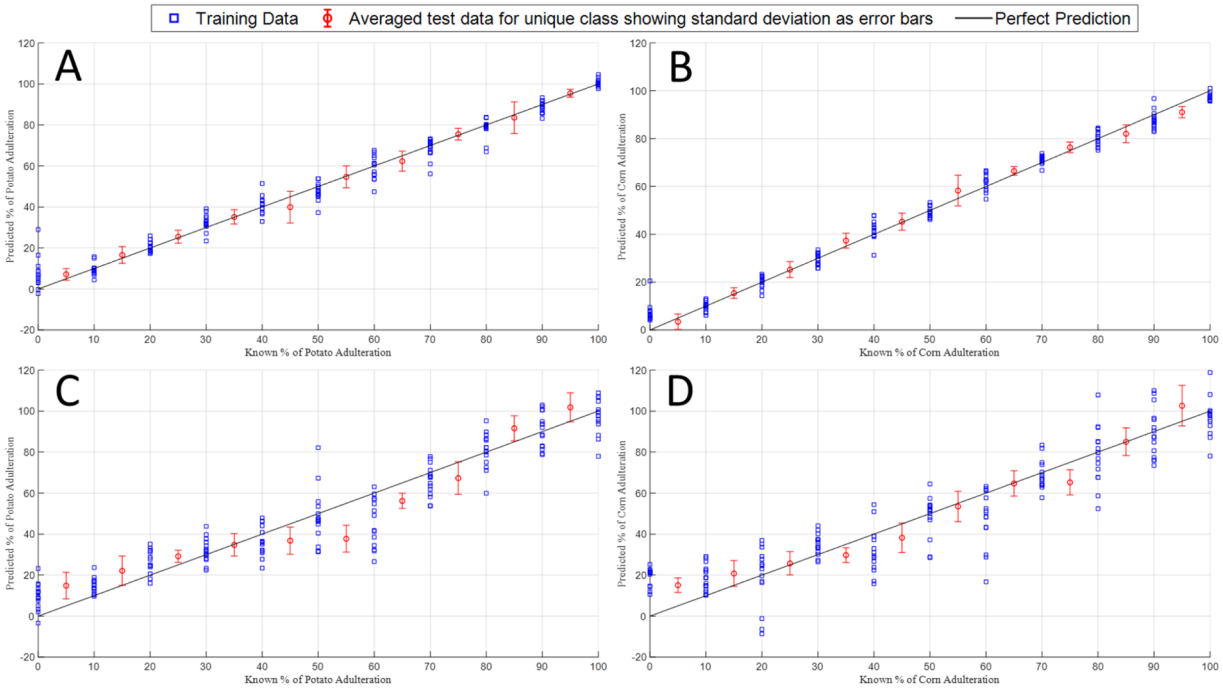


Fig. 4. The results of four PLS-R models trained to predict the levels of corn or potato flour adulterated in wheat flour, built using infrared or Raman spectroscopy. These models include predicting potato adulteration (A) and corn adulteration (B) using infrared data, as well as detecting potato adulteration (C) and corn adulteration (D) using Raman data.

Table 3
Figures of merit for the PLS-R models including R^2, Q^2, RMSECV, RMSEP and LOD.

Flour (Technique)	R^2	Q^2	RMSECV	RMSEP	LOD
Corn (IR)	0.9857	0.9810	3.7804	3.9574	6.9392
Potato (IR)	0.9752	0.9688	4.9754	5.0731	10.0178
Corn (Raman)	0.8364	0.9080	12.7887	8.7116	22.5809
Potato (Raman)	0.8997	0.8649	10.0150	10.5589	25.1717

Where: R^2 and Q^2 show the linearity of predictions for the training and test set, respectively. Also shown are root mean squared error of cross validation (RMSECV) for the training set and root mean squared error of prediction (RMSEP) for the test set. LOD is the limit of detection calculated from the PLS-R models.

inspection alone. These techniques are particularly useful in identifying subtle variations that may otherwise be overlooked in traditional analyses.

3.2.1. PCA of Raman spectroscopy data

The PCA scores plot (Fig. 2A) of Raman data for pure wheat flour adulterated with corn flour and potato flour exhibits a clear trend from right to left as the level of adulteration increases. The positions of the scores for potato and corn along the negative axis of PC-1 are associated with negative bands in the loadings vector of PC-1 (Fig. 2B). Intense negative bands observed at 1380 cm^{-1} and 1391 cm^{-1} can be attributed to polysaccharide deformation modes and C-C-H bending in starch (Table 1), respectively from the adulterant. Another prominent negative band at 862 cm^{-1} is linked to mono-, di-, and polysaccharides, specifically associated with glycosidic bond stretching or deformation modes, again from the increasing level of adulteration with corn and potato flour in wheat flour. These bands serve as reliable indicators of starch presence in the flour samples.

The scores corresponding to wheat flour cluster on the right-hand side of the PCA scores plot, with the positive bands in the PC-1 loadings attributed to wheat components. Notably, a large positive band at 1464 cm^{-1} is observed, which can be assigned to polysaccharides, lipids, and fatty acids (Table 1). However, other studies also identify this band as a strong marker for gluten (Chourpa et al., 2006; Czaja et al., 2016, 2020). This is consistent with the literature, which indicates that corn and potato flours are gluten-free, whereas wheat flour contains gluten (Figure S2 provides a Raman spectrum of gluten). The overlap of the gluten-related band with those of polysaccharides, lipids, and fatty acids may explain the increased intensity of the band observed in wheat flour samples.

3.2.2. PCA of infrared spectroscopy data

The PCA scores of the IR measurements for wheat flour adulterated with corn and potato flour (Fig. 3A) also exhibit a clear trend from right to left as the adulteration level increases. However, unlike for PCA on the Raman spectra, two different trends can be seen for wheat flour adulterated with corn flour (a 9 o'clock trajectory) and for wheat flour adulterated with potato flour (a 7 o'clock trajectory). The scores for pure wheat flour are positioned on the positive side of the PC-1 axis, reflecting the significant influence of positive bands in the PC-1 loadings (Fig. 3B). Two prominent bands in the 1500 cm^{-1} to 1700 cm^{-1} range can be attributed to the β-sheet structures of amide I and amide II, which correspond to protein vibrations related to the peptide bonds (Table 2). As previously discussed, wheat flour has a higher protein content than corn and potato flour, making these bands indicative of wheat flour proteins.

A strong negative band just below 1000 cm^{-1} in the PC-1 loadings is associated with (C—O and C—C) bending vibrations in polysaccharides, particularly starch (Table 2). Corn flour, with the highest starch content among the three, shows scores furthest along the negative side of the PC-1 axis, while pure potato flour scores are positioned between pure corn flour and pure wheat flour of the PC-1 axis. The scores for pure corn and pure potato flours separate along the PC-2 axis as the adulteration level increases. Pure potato flour scores are located on the negative axis of PC-2, and the PC-2 loadings (Fig. 3C) show the key spectral region responsible for this clustering is between 3000 cm^{-1} and 3600 cm^{-1}, attributed to hydroxyl stretching. Variations in this region can be linked to differences in moisture content, starch composition, or even cellulose

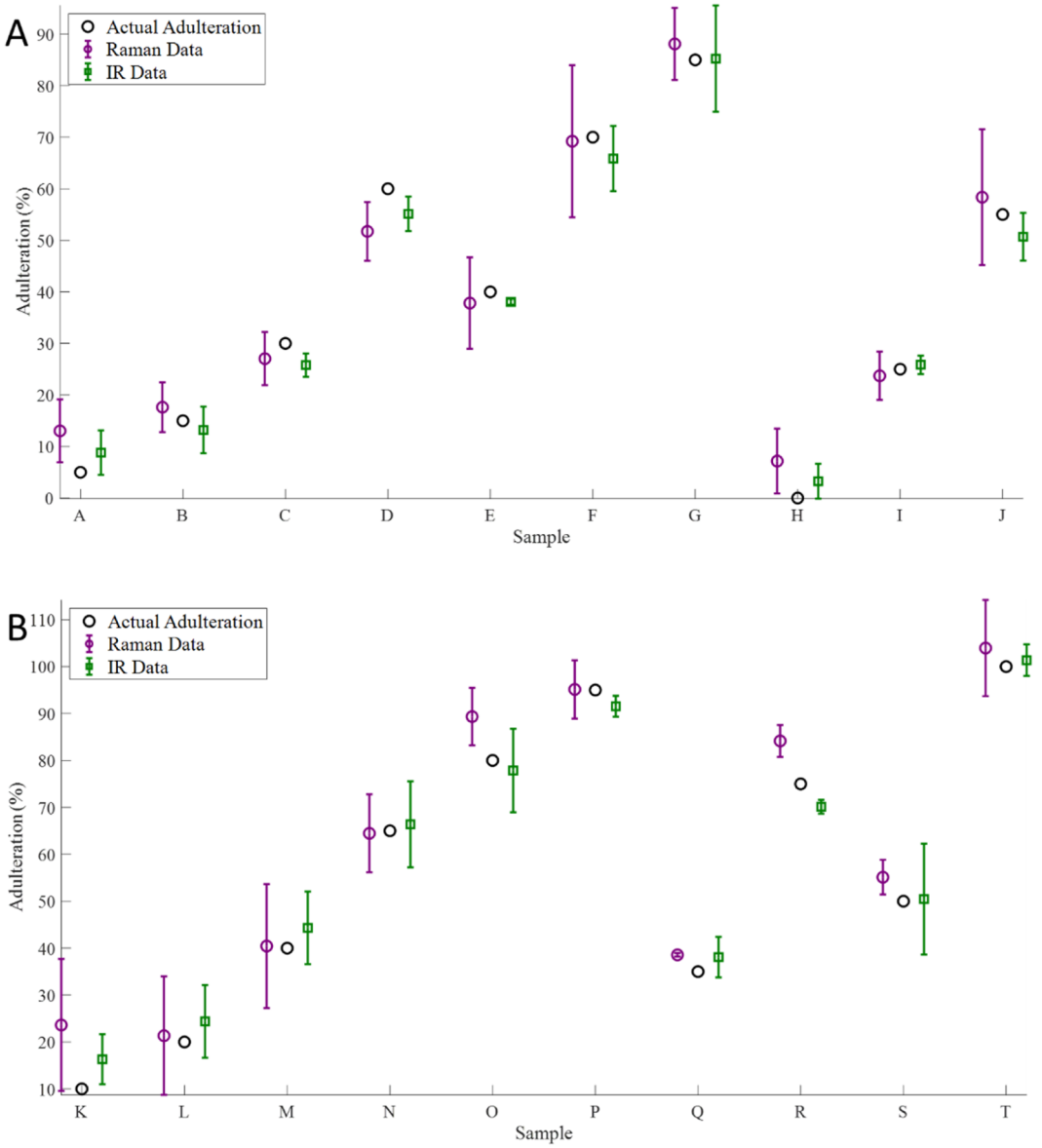


Fig. 5. plots of predicted adulteration levels using Raman and infrared spectroscopy as compared to actual adulteration levels of "blind" samples. Samples A – J represent varying levels of potato flour adulteration in wheat flour (A). Samples K – T represent varying levels of corn flour adulteration in wheat flour (B).

content between the flours.

3.3. *Predicting adulteration levels in wheat flour*

Having established that PCA highlighted there was a systematic change in the Raman and FT-IR data that could be associated with the level of adulteration of wheat flour, we next chose to predict the level of the adulterants using more powerful chemometrics. Partial Least Squares Regression (PLS-R) is effective for predicting adulteration percentages in food samples due to its ability to handle high-dimensional, multivariate data, such as spectral information (Mahesh et al., 2015). It reduces data complexity by extracting latent variables that capture the most variance, enabling accurate predictions despite correlations between compounds. Its versatility across different spectroscopic techniques (e.g., Raman, IR) makes it ideal for detecting adulteration and ensuring quality control in food products. For this study, four PLS-R models were developed to quantify the adulteration of wheat flour with corn and potato flour using both Raman and infrared spectroscopy, as detailed in the Methods.

Fig. 4 shows the PLS-R prediction plots, and Table 3 outlines the figures of merit for the four models, including R^2, Q^2, RMSECV, RMSEP, and LOD. The plots and figures of merit clearly demonstrate that the models perform well for both techniques, with R^2 and Q^2 values close to 1 (1 would show perfect linearity in the predictions for the training (R^2) and test sets (Q^2)) and low RMSECV and RMSEP (i.e., errors in the models for the training and test sets). However, it is evident that the IR-based models outperform the Raman models, exhibiting higher R^2 and Q^2 values, alongside lower RMSECV and RMSEP. This is likely due to Raman being an inherently weak scattering process, while IR spectroscopy relies on absorption, a much stronger interaction, resulting in improved signal-to-noise ratios (Edwards & De Faria, 2004; Muñoz-Bolaños et al., 2024). Additionally, it is important to consider that both spectroscopic techniques involve the analysis of a very limited amount of sample material - often only a small surface area or volume is interrogated in each measurement. This restricted sampling volume means that the PLSR models are built on spectral data representing only a fraction of the total sample, which may not fully capture compositional variability, especially in heterogeneous mixtures. This limitation can affect model robustness and predictive performance if sample preparation is not sufficiently thorough. Ensuring good homogenisation and

Table 4
PLS-R predicted adulteration levels of "blind" samples for Raman and infrared spectroscopy compared to actual adulteration levels. Sample A-J (potato flour adulterated into wheat flour). Sample K-T (corn flour adulterated into wheat flour).

Unknown "Blind" sample	Actual adulteration level (%)	Raman				FT-IR			
		1	2	3	average	1	2	3	average
A	5	17.02	5.99	16.07	13.03	11.76	10.83	3.86	8.82
B	15	21.2	12.14	19.53	17.62	16.84	14.65	8.14	13.21
C	30	23.3	24.90	32.92	27.04	26.26	27.79	23.30	25.78
D	60	45.54	52.86	56.78	51.73	55.23	58.39	51.75	55.12
E	40	37.68	29.02	46.75	37.82	38.71	37.86	37.58	38.05
F	70	85.48	56.65	65.52	69.22	59.30	66.32	71.92	65.85
G	85	96.16	84.15	83.97	88.09	84.81	95.76	75.13	85.23
H	0	10.26	11.32	-0.07	7.17	7.11	1.91	0.75	3.26
I	25	18.34	25.73	27.07	23.71	24.12	25.72	27.69	25.84
J	55	55.01	72.90	47.17	58.36	45.34	53.72	52.97	50.68
K	10	39.64	17.84	13.35	23.61	10.44	17.59	20.90	16.31
L	20	15.23	35.86	12.91	21.33	15.51	28.03	29.61	24.38
M	40	44.91	25.58	50.83	40.44	36.24	45.05	51.65	44.31
N	65	69.31	54.86	69.22	64.46	56.08	73.59	69.50	66.39
O	80	82.26	92.97	92.79	89.34	67.60	82.35	83.63	77.86
P	95	89.69	101.92	93.80	95.14	89.15	91.87	93.57	91.53
Q	35	38.15	38.63	38.92	38.57	33.10	40.43	40.71	38.08
R	75	81.16	87.85	83.46	84.16	69.37	71.83	69.24	70.15
S	50	59.36	52.69	53.28	55.11	45.09	42.25	64.01	50.45
T	100	101.05	115.33	95.47	103.95	98.78	105.17	100.14	101.36

collecting multiple spectra per sample can help mitigate this issue and enhance model reliability.

To calculate the LOD, PLSR models were constructed using only adulteration levels between 5 % and 25 % (in 5 % increments – 10 of the fifteen total spectra at each adulteration level were used as training data and the remaining 5 spectra at each adulteration level were used as test data). This concentration range was chosen because, if an extended range is used the resulting LOD is underestimated, leading to an artificially optimistic assessment of the method's sensitivity. The calculated LOD values were significantly lower for IR spectroscopy (7–10 %) than for Raman (22–25 %), indicating that IR can reliably detect much lower levels of adulteration. It is also important to note that it is generally accepted that economically motivated adulteration is only viable at levels above 20 % (Spinks and Moyer, 2011) so both methods would be useful capable guardians, though infrared would currently be preferred due to its lower LODs and superior model performance.

Having established that infrared and Raman spectroscopy when combined with PLS-R could be used to detect the adulteration of wheat flour with either corn or potato flour, we decided to put the models to the test. Therefore, 20 "blind" samples with known adulteration levels for potato (A-J) or corn (K-T) were prepared by one of us (A.O.), and the same models (trained using data from 0 to 100 % adulteration in 10 % increments) were applied to predict these levels by J.S. The 20 blind samples were run and tested against the four models and the predicted outcomes are displayed in Fig. 5 and summarised in Table 4. Once the code was broken and the actual percentages in the blind samples revealed we found that the predictions of this real test set were excellent. This further highlights the strong performance of the models across both analytical techniques and flour adulterants, with predicted values closely aligning with the actual levels of adulteration. This suggests that the models are robust and can accurately forecast adulteration percentages. A noticeable trend is that Raman data generally exhibits greater variability, as indicated by wider standard deviation error bars, reflecting more fluctuation in the predictions. However, in some instances, the IR data displays higher variability than the Raman data. It should also be noted that the model (Fig. 5A) predicts an average adulteration level of 7.17 % (Raman) and 3.26 % (IR) for sample H, which is pure wheat (contains no adulteration). However, as discussed previously, these values are within the errors calculated from the PLS-R models.

4. Conclusion

This study demonstrates for the first time the effectiveness of portable Raman and infrared spectroscopy for detecting and quantifying the adulteration of wheat flour with potato and corn flour. PCA was able to provide visual identification of varying levels of adulteration, while PLSR models provided accurate predictions of adulterant levels. Calculated LODs also showed that adulteration as low as 6.9 % for IR and 22.6 % for Raman could be reliably detected. These findings highlight the potential of portable vibrational spectroscopy as a rapid, non-destructive tool for food quality monitoring. Given the increasing risk of flour adulteration due to geopolitical instability, such as the war in Ukraine disrupting global grain supplies, proactive monitoring strategies are essential. Implementing portable spectroscopic techniques as capable guardians in supply chains and regulatory frameworks can enhance food fraud detection, ensuring the integrity and safety of wheat flour products.

Acknowledgements

This research was funded by the United Kingdom Research and Innovation (UKRI), Biotechnology and Biological Sciences Research Council (BBSRC), FoodBioSystems Doctoral Training Partnership (FBSDTP), grant number: BB/T008776/.

J.S. and R.G. would like to thank the Nils Foss Excellence Prize for their support. R.G. thanks EPSRC-SFI (EP/V042882/1).

Ethics statement

No human participants or animals were used in this study.

CRediT authorship contribution statement

Abimbola Oluwakayode: Writing – review & editing, Writing – original draft, Visualization, Methodology, Investigation, Formal analysis, Data curation, Conceptualization. **Joe Stradling:** Writing – review & editing, Writing – original draft, Visualization, Methodology, Investigation, Formal analysis, Data curation, Conceptualization. **Angel Medina:** Writing – review & editing, Visualization, Validation, Supervision, Project administration, Methodology, Funding acquisition, Formal analysis, Conceptualization. **Rudolf Krska:** Writing – review & editing, Visualization, Validation, Supervision, Project administration,

Methodology, Funding acquisition, Formal analysis, Conceptualization. **Royston Goodacre:** Writing – review & editing, Visualization, Validation, Supervision, Project administration, Methodology, Funding acquisition, Formal analysis, Conceptualization.

Declaration of competing interest

All authors declare no competing interests.

Supplementary materials

Supplementary material associated with this article can be found, in the online version, at doi:10.1016/j.afres.2026.101913.

Data availability

Data will be made available on request.

References

Arendt, E. K., & Dal Bello, F. (2008). Functional cereal products for those with gluten intolerance. *Technology of Functional Cereal Products*, 446–475.

Arslan, F. N., Akin, G., Karuk Elmas, Ş. N., Üner, B., Yilmaz, I., Janssen, H. G., & Kenar, A. (2020). FT-IR spectroscopy with chemometrics for rapid detection of wheat flour adulteration with barley flour. *Journal of Consumer Protection and Food Safety, 15*, 245–261.

AzoMaterials. (2023) Rapid inline detection of wheat flour adulteration using NIR spectroscopy. [Online][Accessed on 23rd June 2025] https://www.azom.com/article.aspx?ArticleID=22918.

Baker, M. J., Trevisan, J., Bassan, P., Bhargava, R., Butler, H. J., Dorling, K. M., Fielden, P. R., Fogarty, S. W., Fullwood, N. J., Heys, K. A., & Hughes, C. (2014). Using fourier transform IR spectroscopy to analyze biological materials. *Nature Protocols, 9*(8), 1771–1791.

Bansal, S., Singh, A., Mangal, M., Mangal, A. K., & Kumar, S. (2017). Food adulteration: sources, health risks, and detection methods. *Critical Reviews in Food Science and Nutrition, 57*(6), 1174–1189.

Buzera, A., Nkirote, E., Abass, A., Orina, I., & Sila, D. (2023). Chemical and pasting properties of potato flour (Solanum tuberosum L.) in relation to different processing techniques. In *Journal of Food Processing and Preservation, 2023*, Article 3414760.

Chien, H. J., Zheng, Y. F., Wang, W. C., Kuo, C. Y., Hsu, Y. M., & Lai, C. C. (2023). Determination of adulteration, geographical origins, and species of food by mass spectrometry. *Mass Spectrometry Reviews, 42*(6), 2273–2323.

Choudhary, A., Gupta, N., Hameed, F., & Choton, S. (2020). An overview of food adulteration: concept, sources, impact, challenges and detection. *International Journal of Chemical Studies, 8*(1), 2564–2573.

Chourpa, I., Ducel, V., Richard, J., Dubois, P., & Boury, F. (2006). Conformational modifications of α gliadin and globulin proteins upon complex coacervates formation with gum arabic as studied by Raman microspectroscopy. *Biomacromolecules, 7*(9), 2616–2623.

Czaja, T., Mazurek, S., & Szostak, R. (2016). Quantification of gluten in wheat flour by FT-Raman spectroscopy. *Food Chemistry, 211*, 560–563.

Czaja, T., Sobota, A., & Szostak, R. (2020). Quantification of ash and moisture in wheat flour by Raman spectroscopy. *Foods (Basel, Switzerland), 9*(3), 280.

Edwards, H. G., & De Faria, D. L. (2004). Infrared, Raman microscopy and fibre-optic Raman spectroscopy (FORS). *Non-Destructive Microanalysis of Cultural Heritage Materials. Elsevier, The Netherlands, 42*, 359–395.

Ellis, D. I., Brewster, V. L., Dunn, W. B., Allwood, J. W., Golovanov, A. P., & Goodacre, R. (2012). Fingerprinting food: current technologies for the detection of food adulteration and contamination. *Chemical Society Reviews, 41*(17), 5706–5727.

Ellis, D. I., Muhamadali, H., Allen, D. P., Elliott, C. T., & Goodacre, R. (2016). A flavour of omics approaches for the detection of food fraud. *Current Opinion in Food Science, 10*, 7–15.

Essuman, E. K., Teye, E., Dadzie, R. G., & Sam-Amoah, L. K. (2022). Consumers' knowledge of food adulteration and commonly used methods of detection. *Journal of Food Quality, 2022*(1), Article 2421050.

Faller, A. C., Kesanakurti, P., & Arunachalam, T. (2021). Fraud in grains and cereals. *Food fraud* (pp. 281–308). Academic Press.

Gautam, R., Vanga, S., Ariese, F., & Umapathy, S. (2015). Review of multidimensional data processing approaches for Raman and infrared spectroscopy. *EPJ Techniques and Instrumentation, 2*, 1–38.

King Arthur Baking. (2017). *How to substitute for potato flour* [Online] [Accessed on 15th January 2025] https://www.kingarthurbaking.com/blog/2017/11/17/how-to-substitute-for-potato-flour.

Li, S., Li, T., Cai, Y., Yao, Z., & He, M. (2024). Rapid quantitative analysis of rongalite adulteration in rice flour using autoencoder and residual-based model associated with portable Raman spectroscopy. *Spectrochimica Acta Part A: Molecular and Biomolecular Spectroscopy, 304*, Article 123382.

Lohumi, S., Lee, H., Kim, M. S., Qin, J., & Cho, B. K. (2019). Raman hyperspectral imaging and spectral similarity analysis for quantitative detection of multiple adulterants in wheat flour. *Biosystems Engineering, 181*, 103–113.

Mahesh, S., Jayas, D. S., Paliwal, J., & White, N. D. G. (2015). Comparison of partial least squares regression (PLSR) and principal components regression (PCR) methods for protein and hardness predictions using the near-infrared (NIR) hyperspectral images of bulk samples of Canadian wheat. *Food and Bioprocess Technology, 8*, 31–40.

Meghwal, M., Mahalakshmi, M., Mahalakshmi, R., Rani, S., de Souza, C. K., Jain, S., Ojha, A., Kumar, N., Katariya, L., Meghwal, K., & Mahalakshmi, S. (2022). Food adulteration: A challenge for safer food. *Food safety practices in the restaurant industry* (pp. 221–254). IGI Global.

Muñoz-Bolaños, J. D., Rajaeipour, P., Kummer, K., Kress, M., Ataman, Ç., Ritsch-Marte, M., & Jesacher, A. (2024). Confocal raman microscopy with adaptive optics. *ACS Photonics,, 12*(1), 176–184.

Narayan, D. (2014). Food adulteration: types, worldwide laws and futures. *Health Care, 1*, 2–8.

Oliveira, M. M., Cruz-Tirado, J. P., Roque, J. V., Teófilo, R. F., & Barbin, D. F. (2020). Portable near-infrared spectroscopy for rapid authentication of adulterated paprika powder. *Journal of food composition and analysis, 87*, Article 103403.

Pastor, K., Ačanski, M. and Vujić, D. (2019) Gas chromatography in food authentication. *Gas chromatography-derivatization, sample preparation, application*, p.109.

Reliefweb. (2024) Ukraine - wheat flour and sunflower oil value chains: analysis of value chains with a focus on smaller farmers and processors near the frontline, April 2024 [Online][Accessed on 23rd May 2025]. https://reliefweb.int/report/ukraine/ukraine-wheat-flour-and-sunflower-oil-value-chains-analysis-value-chains-focus-smaller-farmers-and-processors-near-frontline-april-2024.

Tomar, P., & Alka, G. (2022). Food adulteration and its impact on health. *International Journal of Home Science, 8*(2), 164–168.

Sahu, P. K., Panda, J., Jogendra Kumar, Y. V. V., & Ranjitha, S. K. (2020). A robust RP-HPLC method for determination of turmeric adulteration. *Journal of Liquid Chromatography & Related Technologies, 43*(7-8), 247–254.

Savitzky, A., & Golay, M. J. (1964). Smoothing and differentiation of data by simplified least squares procedures. *Analytical Chemistry, 36*(8), 1627–1639.

Sezer, B., Unuvar, A., Boyaci, I. H., & Köksel, H. (2022). Rapid discrimination of authenticity in wheat flour and pasta samples using LIBS. *Journal of Cereal Science, 104*, Article 103435.

Stawoska, I., Wesełucha-Birczyńska, A., Skoczowski, A., Dziurka, M., & Waga, J. (2021). FT-raman spectroscopy as a tool to study the secondary structures of wheat gliadin proteins. *Molecules (Basel, Switzerland), 26*(17), 5388.

Stradling, J., Muhamadali, H., & Goodacre, R. (2024). Mobile guardians: detection of food fraud with portable spectroscopy methods for enhanced food authenticity assurance. *Vibrational Spectroscopy, 132*, Article 103673.

Unuvar, A., Boyaci, I. H., Yazar, S., & Koksel, H. (2023). Rapid detection of common wheat flour addition to durum wheat flour and pasta using spectroscopic methods and chemometrics. *Journal of Cereal Science, 109*, Article 103604.

Van Hung, P., Maeda, T., & Morita, N. (2006). Waxy and high-amylose wheat starches and flours—Characteristics, functionality and application. *Trends in Food Science & Technology, 17*(8), 448–456.

Ziegler, J. U., Leitenberger, M., Longin, C. F. H., Würschum, T., Carle, R., & Schweiggert, R. M. (2016). Near-infrared reflectance spectroscopy for the rapid discrimination of kernels and flours of different wheat species. *Journal of Food Composition and Analysis, 51*, 30–36.



https://dspace.org/

Detecting wheat flour adulteration by portable infrared and Raman spectroscopies

Oluwakayode, Abimbola; Stradling, Joe; Medina, Angel; Krska, Rudolf; Goodacre, Royston

2026-06
Elsevier
https://doi.org/10.1016/j.afres.2026.101913
Oluwakayode A, Stradling J, Medina A, et al., (2026) Detecting wheat flour adulteration by portable infrared and Raman spectroscopies. Applied Food Research, Volume 6, Issue 1, June 2026, Article number 101913

Downloaded from a DSpace repository. https://dspace.org/